19 Mar 2001

Statistical Characterization of Macroscale Multiphase Flow Textures in Trickle Beds

Y. Jiang

M. (Muthanna) H. Al-Dahhan
Missouri University of Science and Technology, aldahhanm@mst.edu

M. P. Duduković

Recommended Citation

Y. Jiang et al., "Statistical Characterization of Macroscale Multiphase Flow Textures in Trickle Beds," *Chemical Engineering Science*, vol. 56, no. 4, pp. 1647 - 1656, Elsevier, Mar 2001.
The definitive version is available at https://doi.org/10.1016/S0009-2509(00)00393-6

PERGAMON

Chemical Engineering Science 56 (2001) 1647–1656

Chemical Engineering Science

www.elsevier.nl/locate/ces

Statistical characterization of macroscale multiphase flow textures in trickle beds

Y. Jiang[1], M. H. Al-Dahhan*, M. P. Duduković

Chemical Reaction Engineering Laboratory (CREL), Department of Chemical Engineering, Washington University, St. Louis, MO 63130, USA

Abstract

Experimental studies (Lutran et al., Ind. Engng Chem. Res. 30 (1991) 1270; Ravindra et al., Ind. Engng Chem. Res. 36 (1997) 5133) and numerical simulation (Jiang et al., Chem. Engng Sci. 54 (1999) 2409–2419) lead to the conclusion that fluid flow distribution in trickle beds is a function of bed structure (i.e. porosity distribution), particle external wetting and inlet superficial velocities of the two fluids. In this study, quantitative relationships among the above parameters are developed in a statistical manner through a series of computational fluid dynamics simulations. The contribution of capillary forces to liquid maldistribution is significant in the case of partial particle external wetting; however, it is shown that the effect of porosity non-uniformity in packed beds can be reduced if the particles are prewetted well.

Keywords: Trickle beds; Flow distribution; Multiscale flow; Statistical hydrodynamics; Moments; CFD

1. Introduction

For successful scale-up and design of trickle beds, it is important to understand and predict the complex multiphase fluid dynamics. In other words, one needs to know, how the hydrodynamic quantities such as phase holdup, gas and liquid velocities and phase pressure are distributed spatially and temporally in the multi-dimensional reactors. Even the precise description of the steady-state hydrodynamics requires not only the information on global quantities (i.e., overall holdup and pressure drop), which can be calculated primarily by empirical or phenomenological models (Saez & Carbonell, 1985; Holub, Dudukovic & Ramachandran, 1992,1993), but also the information on the distribution of these quantities. Both experimental studies (Lutran, Ng & Delikat, 1991; Ravindra, Rao & Rao, 1997) and numerical simulation (Jiang, Khadilkar, Al-Dahhan & Dudukovic, 1999) lead to the conclusion that fluid-flow distribution under steady-state condition is a function of bed structure (i.e., porosity distribution), particle wetting and the inlet superficial velocities of the two phases. However, there is no quantitative relationship available in the literature to describe the state of the bed and its effect on reactor performance.

To develop such a model, one needs to first understand the nature of the system. Fortunately, recent experiments revealed that the fluid-velocity distribution (Sederman, Johns, Bramley, Alexander & Gladden, 1997; Volkov, Reznikov, Khalilov, Zel'vensky & Sakodynsky, 1986), liquid holdup distribution (Toye, Marchot, Crine & L'Homme, 1997) and porosity distribution (Chen, Rodas, Al-Dahhan & Dudukovic, 2000) in packed beds are pseudo-random in nature. This means that the local hydrodynamic quantities (such as holdups and velocities as well as particle external wetting efficiency) and local porosity can be considered as random variables. The global hydrodynamics then can be described by the local hydrodynamic parameters through a proper probability density function (Crine, Marchot & L'Homme, 1992). The goal of this study was to search for such a probability function and to describe the function parameters in terms of measurable parameters such as bed dimensions, particle size and shape, operating conditions, etc.

The logical way to pursue this goal is to conduct extensive measurements of the bed-scale hydrodynamics and of the local-scale hydrodynamic parameters, simultaneously. This requires the determination of bed structure characteristics, such as porosity distribution, with the same spatial resolution as achieved in flow measurements. Although the non-invasive tomography techniques are available for such high-cost experiments (Toye et al., 1997; Sederman et al., 1997; Reinecke, Petritsch, Schmitz & Mewes, 1998), the numerical flow simulation

* Corresponding author.

[1] *Current address:* Conoco Inc., 1000 South Pine St., RW6685, Ponca City, OK 74604-1267, USA.

E-mail address: muthanna@wuche.wustl.ed (M. H. Al-Dahhan).

0009-2509/01/$ - see front matter
PII: S0009-2509(00)00393-6

provides also a rational way, with good cost-effectiveness, to obtain useful preliminary results needed to guide the future experimental validation study.

To effectively model the gas and liquid distributions in trickle beds, one should resolve two critical issues: (i) how to implement the complex geometry of the packed bed in the flow equations (*structure problem*); (ii) how to take into account the gas–liquid–solid interactions (*closure problem*). Most previous approaches 'solved' these two problems in a simplistic manner. For bed structure problem one used either the mean porosity, or the longitudinally averaged porosity profile (i.e. an oscillating radial porosity profile, $\varepsilon(r)$) or the mean porosity with some empirical quantities (e.g. radial spreading factor, effective viscosity, effective diffusivity) (Song, Yin, Chuang & Nadakumar, 1998; Bey & Eigenberger, 1997). Recently, for the purpose of heat-transfer study of gas flow in a single tube fixed-bed with low tube-to-particle diameter ratio (2–3), a 3D computational fluid dynamics (CFD) simulation was performed by generating the fine mesh within the interstitial void space between particles of large size (~ 5 cm) (Logtenberg & Dixon, 1998; Nijemeisland, Logtenberg & Dixon, 1998). It is impossible, however, for a massive commercial column, or even for a bench-scale trickle bed with small particle size (0.5–3 mm) to use such fine-mesh approach. Moreover, it is also not necessary because the exact porosity structure is completely changed with re-packing even with the same particles and the same packing method. However, we should be able to obtain the same or similar statistical quantities of the bed porosity distribution even after re-packing. Thus, one can generate a porosity distribution with same statistical characteristics under certain constraints, and then use such porosity distribution section by section in further numerical flow simulation.

Closure problem is the second tough issue in multiphase flow simulation. The existence of microscopic turbulence in porous media has been detected by several experiments by point-wise probes (Jolls & Hanratty, 1966; Latifi, Midoux & Storck, 1989); therefore, one has to take Reynolds stress term into consideration in the fine-mesh CFD modeling with high gas flow rate (see Nijemeisland et al., 1998). For the macroscale flow modeling in packed beds, however, the contribution of the Reynolds stress term to the fluid momentum equation is not important (Jiang, Khadilkar, Al-Dahhan & Dudukovic, 2000) because when averaging a number of local (random) signals within a representative elementary volume (e.g., a cubic section containing a cluster of particles), the microscopic turbulence is smoothed out. In fact, the interfacial momentum exchange terms play a significant role in multiphase flow simulations. The capillary pressure caused by the gradient of phase holdup and particle partial wetting can generate pressure differences between the gas and the liquid phase. Such pressure difference can affect the fluid flow distribution significantly, as confirmed by experimental observations of liquid distribution (Ravindra et al., 1997; Jiang et al., 1999) and flow simulation by the extended discrete cell model (DCM) (Jiang et al., 1999).

In this paper, we focus on modeling the macroscale flow distribution in trickle beds by implementing the statistical porosity structure and by modeling the complex multiphase interacting forces in the flow equations. By analyzing a series of bed structures and flow simulation results, we develop the preliminary statistical correlations for the structure-flow relationship.

2. Statistical nature of bed structure and flow

2.1. Bed structure

The porosity and its distribution in a packed bed are the key parameters in determining the flow distribution. The effective implementation of porosity distribution in the flow simulation model is the critical point, which affects the capability and applicability of the developed flow model. To achieve a quantitative understanding of the porosity distribution in packed beds, numerous research efforts have been made during the past several decades. For instance, measurements of the longitudinally averaged radial porosity profiles (Benenati & Brosilow, 1962), correlations of radial porosity distribution (Mueller, 1991; Bey & Eigenberger, 1997) and sphere-packing computer simulation of 3-D porosity structure (Jodrey & Tory, 1981), etc. have been reported. It was found that the mean porosity and porosity distribution are determined largely by particle size, shape, and particle surface properties (i.e. roughness and hardness) as well as the method of packing the bed.

The recent advances in computer tomography (CT) and magnetic resonance imaging (MRI) techniques can provide the 3-D structure in packed beds in a non-invasive way (Reinecke et al., 1998; Baldwin, Sederman, Mantle, Alexander & Gladden, 1996). Depending on the spatial resolution of the techniques used, different types of porosity distributions were found. For instance, the porosity data obtained from γ-ray CT scans of a cylindrical column packed with 3-mm monosize spheres has definitely exhibited a Gaussian distribution of the pixel porosity values at a pixel size (i.e., spatial resolution) of 4 mm (Chen et al., 2000). However, it has been found by MRI that there are two peaks in the distribution of voxel porosity values of the bed with 3 mm particles if the voxel size is reduced to 180 μm (Sederman, 2000): one with low value due to voxels filled with solid and one high value due to voxels filled with pore space. This implies that the type of porosity distribution depends on the size of voxel (or pixel size) chosen in the measurements. In general, the porosity distribution is certainly Gaussian if the voxel size is larger than the particle diameter. In this study we

focus on the modeling of macroscale flow texture, which is on the scale of a cluster of particles.

2.2. Multiscale flow and multi-force actions

Due to the mixed definitions encountered in the literature, it is necessary to clearly define each spatial scale referred to in this paper.

- *Microscale level*: the scale of interstitial space (< particle diameter), also called 'local scale' or 'particle scale'.
- *Mesoscale level*: The scale of a cluster of particles, also called 'section scale'.
- *Macroscale level*: the scale of an elementary volume large enough to be representative of the bed (Crine et al., 1992), also called 'large scale' or 'bed scale'.

The experimental observations in packed beds have also shown that the fluid flow distribution is multiscale in nature, and flow distribution/maldistribution can be observed from the macroscale to the microscale (Hoek, Wesselingh & Zuiderweg, 1986; Melli, Santos, Kolb & Scriven, 1990; Wang, Mao & Chen, 1998). From flow modeling point of view, it means that, to describe the different scales of flow textures, one needs to implement the governing flow equations with the different details of basic-forces (i.e., inertial, viscous, capillary, and gravitational force, etc.). As we found earlier (Jiang et al., 2000), the contribution of the Reynolds stress term to the fluid momentum equations is not important for the 'macroscale' flow modeling, but it should be very important for the 'microscale' flow simulation (Nijemeisland et al., 1998). On the other hand, also depending on the scale of packing elements used in the packed beds, which essentially determine the scale of flow passages, the contributions of each basic-force on liquid flow distribution are of different magnitudes (Melli et al., 1990). In the beds packed with large packing elements (e.g., separation packing: 10–30 mm Pall rings and Rasching rings etc.) the liquid distribution patterns are not sensitive to the wetability of the packing surface (Bemer & Zuiderweg, 1978). For the trickle-bed packing: typically, 0.5–3 mm spherical or cylindrical particles, however, the influences of particle wetting on liquid distribution are significant (Levec, Saez & Carbonell, 1986; Lutran et al., 1991; Ravindra et al., 1997; Jiang et al., 1999). This implies that even for the same macroscale flow texture (e.g. macroscale-flow distribution), the contribution of each basic force is of different magnitude depending on the different characteristic radius of the flow passages.

2.3. Link of macroscale and cell-scale hydrodynamics

Because the multiscale spectrum of flow-fluid textures exists in multiphase flow packed beds, two critical questions are raised accordingly: (i) '*what is the fundamental mechanism that links those different scales of flow textures in packed beds*?' (ii) '*Is it realistic to develop a universal flow model which can capture the whole spectrum of flow structures*?'

The experimental evidence (Melli et al., 1990) and relevant theoretical study (Melli & Scriven, 1991) have shown that in a nearly 2-D network, the macroscale-flow regimes can be described in terms of different combination of microscale flow regimes. That means that the microscale and meso-scale hydrodynamics in packed beds are the roots of global hydrodynamics. Theoretically, one can link the macroscale and micro- or meso-scale flow textures through certain rules. Crine et al. (1992) introduced the concept of statistical hydrodynamics, in which all the local hydrodynamic quantities were considered as random variables, like the packing properties discussed in Section 2.1. Then the link of the bed scale, section scale and local scale hydrodynamics is the probability density function (p.d.f.) of the random variables, through which the global hydrodynamic quantities can be determined at the bed scale.

In this paper we start from 'section scale' (i.e., meso-scale) flow and structure elements, and examine how the section scale flow hydrodynamics is affected by the section scale bed structure and relevant basic-forces. We then seek the link which bridges the bed scale (i.e., global) and section scale hydrodynamics in a statistical manner.

2.4. Statistical quantities

Since the section scale flow and porosity are random in nature in packed beds, one can use certain statistical methodology to characterize such randomness of the system. The relevant quantities can be described by a probability density function (p.d.f.) characterized by its moments such as mean (μ), variance (σ^2), skewness (γ_1) and kurtosis (γ_2). The definitions of these are readily available in the literature (Roussas, 1997). In this work, we will use the mean, μ

$$\mu = \sum_j x_j p(x_j), \tag{1}$$

where $p(x_j)$ is the probability density function of the random variable x_j of the system, and the variance, σ^2

$$\sigma^2 = \sum_j (x_j - \mu)^2 p(x_j) \tag{2}$$

can be used to characterize the spread around the mean. We examine the effect of skewness and kurtosis on the results also, since the two values of these would indicate the changes caused by a non-Gaussian probability density function.

3. Multiphase flow modeling in trickle beds

In this work the ensemble averaged k-fluid model in the computational fluid dynamics code, CFDLIB, developed by Los Alamos National Laboratory (Kashiwa, Padial, Rauenzahn & Vander Heyden, 1994) is used as a transient multiphase flow simulation tool, which has been adopted for trickle beds, and can handle gas and liquid two-phase flow with stationary solid phase (Kumar, 1995; Khadilkar, 1998; Jiang et al., 1999). Here we provide only the key aspects of the flow equations and the relevant closure formulations for the case of trickle-bed reactors.

Equation of continuity:

$$\frac{\partial \rho_k}{\partial t} + \nabla \rho_k u_k = 0. \tag{3}$$

Equation of momentum:

$$\frac{\partial \rho_k u_k}{\partial t} + \nabla \rho_k u_k u_k = F_{D(k-l)} + \rho_k g + \theta_k \nabla p - \nabla \langle \alpha_k \rho_0 u'_k u'_k \rangle. \tag{4}$$

The momentum exchange term, $F_{D(k-l)}$, is expressed as a product of the exchange coefficient, X_{kl}, phase volume fractions, and relative velocity of the two phases k and l as shown below:

$$F_{D(k-l)} = \theta_k \theta_l X_{kl} (u_k - u_l) \tag{5}$$

X_{kl} is calculated by the modified two-phase flow Ergun equation (Holub et al., 1992) in which constant Ergun parameters are used ($E_1 = 180$, $E_2 = 1.8$). The discussion regarding choosing constant Ergun parameters is given elsewhere (Jiang et al., 2000). Therefore, the exchange coefficient between the liquid and solid phase (X_{ls}) and the gas and solid phase (X_{gs}) can be written as

$$X_{ks} = (A_{ks}\, \mu_k V_k + B_{ks} \rho_k V_k^2) \frac{1}{(1-\varepsilon)|u_k|}, \tag{6a}$$

$$A_{ks} = 180 \frac{(1-\varepsilon)^2}{\theta_k^3 d_p^2}, \tag{6b}$$

$$B_{ks} = 1.8 \frac{(1-\varepsilon)}{\theta_k^3 d_p}. \tag{6c}$$

For gas–liquid drag, either no interaction is assumed for the low-interaction regime or the drag coefficient derived from two-fluid interaction model (Attou, Boyer & Ferschneider, 1999) is used:

$$X_{gl} = \frac{\theta_g}{\varepsilon} (A_{gl} \mu_g V_r + B_{gl} \rho_k V_r^2) \frac{1}{(1-\varepsilon)|u_g - u_l|}, \tag{7a}$$

$$A_{gl} = 180 \frac{(1-\theta_g)^2}{\theta_g^3 d_p^2} \left(\frac{1-\varepsilon}{1-\theta_g} \right)^{2/3}, \tag{7b}$$

$$B_{gl} = 1.8 \frac{(1-\theta_g)}{\theta_g^3 d_p} \left(\frac{1-\varepsilon}{1-\theta_g} \right)^{1/3}, \tag{7c}$$

$$V_r = \theta_g |u_g - u_l|. \tag{7d}$$

The influence of phasic pressure differences due to the interfacial tension and the gradient of liquid volume fraction, which reflects the contribution of the capillary force on the liquid-flow distribution, is also taken into account in pressure calculations by Eq. (8). This equation was proposed by Grosser, Carbonell and Sundaresan (1988) and modified by Jiang et al. (1999) by introducing the particle external wetting factor, f, which can be evaluated by the correlation for particle external wetting efficiency (Al-Dahhan & Dudukovic, 1995):

$$p_L = p_G - (1-f) \frac{(1-\varepsilon) E_1^{0.5}}{\varepsilon d_p} \sigma_s \times \left[0.48 + 0.036 \ln \left(\frac{\varepsilon - \theta_L}{\theta_L} \right) \right]. \tag{8}$$

The Reynolds stress term ($\nabla \langle \alpha_k \rho_0 u'_k u'_k \rangle$) is negligible for the case discussed in this paper.

4. Numerical simulation results and discussions

As discussed in Sections 1 and 2, the observed flow textures in trickle beds result from a combination of interstitial structure (porosity distribution), interaction of between the fluids and particles and the interaction of between the gas and the liquid phase. In this study, we examine each individual contribution to two-phase flow distribution by performing a series of numerical experiments. The following issues are addressed: (i) how does the capillary force affect the flow distribution? (ii) how is the flow distribution affected by porosity distribution? (iii) what is the influence of superficial velocities at the inlet?

4.1. Model packed beds

Recall that the type of porosity distribution in packed beds is scale-dependent. A pseudo-Gaussian distribution of porosity at a section scale (5–10 mm) can be considered as a reasonable assumption for section-scale flow simulation in trickle beds.

A 2-D rectangular model bed of dimensions 50 cm × 10 cm was considered with pre-assigned porosity values to different sections (50 sections in the vertical (z) direction and 10 sections in the horizontal (x) direction as shown in Fig. 1).

The generated pseudo-Gaussian porosity distributions have the same mean value ($\mu \sim 0.40$) but have different standard deviation (S.D.), skewness (γ_1) and kurtosis (γ_2) as listed in Table 1. The gas and liquid flow were

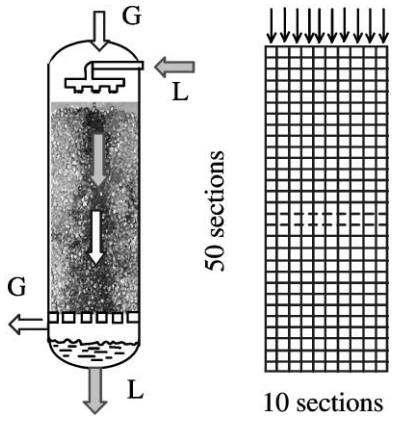

Fig. 1. Trickle bed and model bed with 500 sections ($d_p = 3$ mm).

Table 1
Statistical quantities of porosity distribution

Beds	Mean (μ)	S.D. (σ)	Skewness (γ_1)	Kurtosis (γ_2)
I	0.399	0.0082	0.2736	0.1335
II	0.399	0.0118	− 0.2093	0.6746
III	0.399	0.0217	0.0351	0.0203
IV	0.404	0.0439	− 0.1128	− 0.2972

introduced at the top of the bed at certain superficial velocities. The fluid system used in the simulations is air and water, but any type of system such as hydrogen and hydrocarbons can be simulated by changing physical properties of the fluids. Atmospheric pressure is considered in this study but high-pressure can be handled by using different physical properties and high-pressure formulations for the drag coefficients.

4.2. Capillary force effect

To examine the effect of capillary force on the two-phase flow distribution in a packed bed, a series of CFDLIB simulations have been performed by incorporating a particle wetting factor (f) in the k-fluid pressure calculation (see Eq. (8)). Two limiting wetting conditions are defined, namely, 'complete prewetting' and 'complete non-prewetting'. The actual situation of particle wetting in trickle beds is somewhere between these two limits. The 'complete prewetting' means that there is always a liquid film covering all the particle surfaces, this results in the negligible effect of capillary force on liquid flow. Correspondingly, capillary pressure is not accounted for in flow computation by assigning a value of unity for f. Strictly speaking, this does not happen in practice, even if one pre-wets the bed at high gas- and liquid-flow rates before starting to operate the trickle bed. One often drains the liquid from the bed after terminating the liquid and gas flow (Levec, Grosser & Carbonell, 1988). On draining, the liquid films over the particles, connecting the pendular rings, might rupture, leaving isolated pendular rings at the contact points of the particles. It is argued by Ravindra et al. (1997) that the bed with isolated pendular rings, especially with large diameter particles, could behave as a non-prewetted bed. On the other hand, 'completely non-prewetted' bed means there is no liquid film over the particles, then capillary force fully contributes to the liquid flow distribution. Accordingly, capillary pressure is fully incorporated into CFDLIB computation by assigning to f the value of zero. By changing the wetting factor (f) from 0.0 to 0.5 and 1.0, one can study the effect of capillary force on flow distribution in completely non-prewetted, partially prewetted and completely prewetted beds, respectively.

Fig. 2 shows the simulated longitudinal profiles of porosity, liquid holdup and liquid saturation at different wetting factors ($f = 0$, 0.5 and 1.0). Here the section liquid saturation is defined as the ratio of the section liquid holdup and section porosity. In the completely non-prewetted bed ($f = 0.0$), the liquid saturation profile and porosity profile in the longitudinal direction (z) have similar trends. Lower liquid saturation occurs in lower porosity regions (see Fig. 2a). This can be explained by

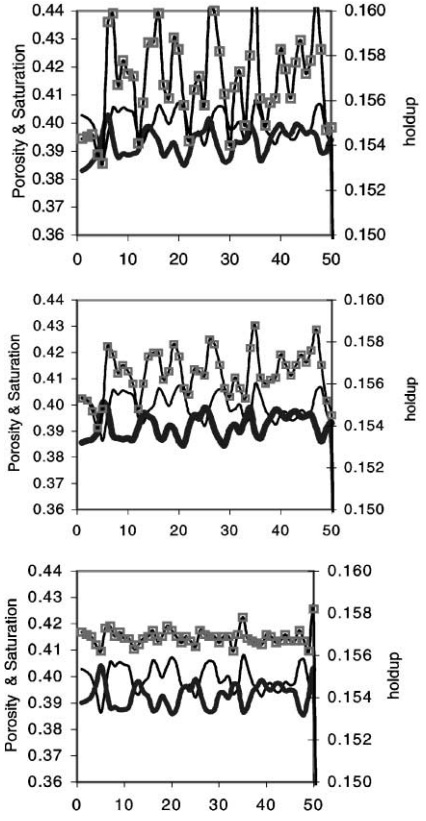

Fig. 2. Transverse averaged profiles of porosity (hard line), liquid holdup (line with square) and liquid saturation (thin line) vs. longitudinal position (z) at different wetting states (a) $f = 0.0$; (b) 0.5; (c) 1.0 at $U_l = 0.3$ cm/s, $U_g = 6.0$ cm/s,

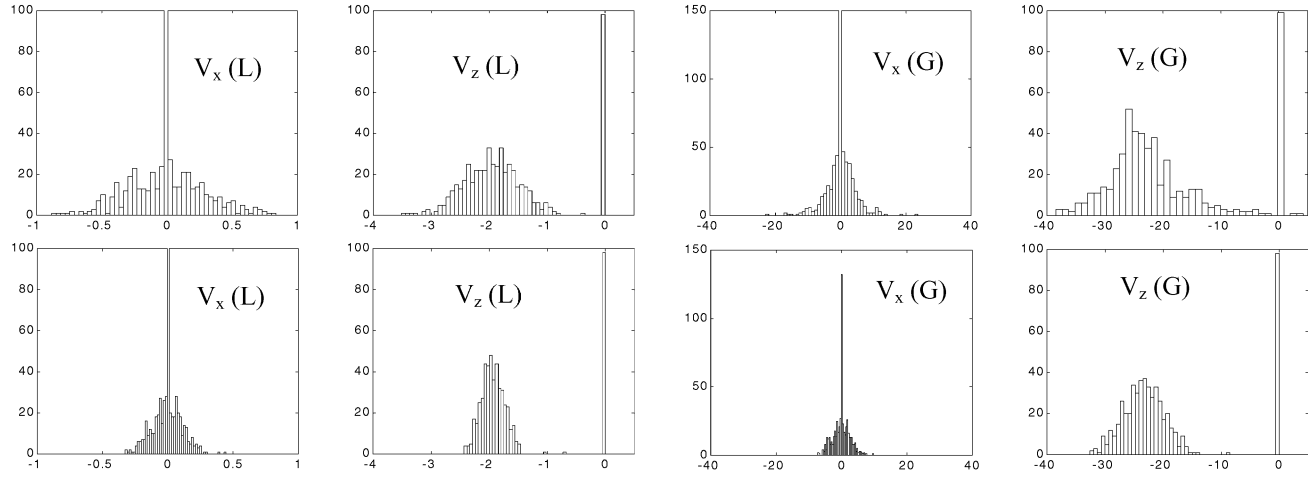

Fig. 3. Distribution of gas and liquid interstitial velocity components in non-prewetted bed ($f = 0$) (upper-row plots) and in prewetted bed ($f = 1$) (lower-row plots) at $U_{l0} = 0.3$ cm/s, $U_{g0} = 6.0$ cm/s (G-gas, L-liquid) (unit in cm/s).

higher capillary force occurring at smaller interslice when the particle surface is non-prewetted. Because the section liquid holdup is a product of the section porosity and section liquid saturation, the variation of liquid holdup is more pronounced than the variation of porosity. When the wetting factor, f, increases, the capillary force effect becomes less significant.

For the case of completely prewetted particles, liquid occupies the low porosity regions with higher liquid saturation. The liquid saturation profile and the porosity profile now have opposite trends as shown in Fig. 2c. The variation of liquid holdup in the longitudinal direction, then, becomes small. Similar results are obtained for the lateral profiles of liquid saturation at different wetting factors indicating that completely prewetted particles can diminish the effect of local porosity variation on liquid distribution and improve liquid holdup distribution.

Histograms showing the distribution of the gas and liquid velocity components are displayed in Fig. 3. The distribution in horizontal velocity components V_x(L) and V_x(G) in a prewetted bed (upper row in Fig. 3) and non-prewetted bed (lower row in Fig. 3) are, as expected, symmetric about zero velocity, but higher standard deviations of V_x(L) and V_x(G) are found in the non-prewetted bed. The distribution for vertical velocity components, V_z(L) and V_z(G), are Gaussian in nature, and almost symmetric about the mean value. The observed zero velocities of the vertical velocity components V_z(L) and V_z(G) are due to the no-slip boundary condition used for left and right walls of the model beds. As the z-axis points upward the axial downward velocities are negative. It is of interest to note that in the case of non-prewetted beds some positive axial velocity component V_z(G) exist, indicating counter-current gas flow is observed locally (see Fig. 3 — up — right). This may be explained by the high heterogeneity of liquid holdup which occurs in the non-prewetted bed due to capillary force. This implies that the effect of liquid maldistribution on gas flow distribution in trickle bed can be significant, especially in non-prewetted beds. The positive local gas velocity leading to local counter-current flow of gas and liquid may explain why in the high interaction regime the slit model of Holub et al. (1992) needed to be modified by Al-Dahhan, Khadilkar, Wu and Dudukovic (1998) to include a 'negative' slip between gas and liquid at the gas–liquid interface.

4.3. Porosity distribution effect

To examine the porosity distribution effect, the beds with the same mean porosity but with different standard deviations (S.D.) of the porosity distribution (see Table 1) are used in the k-fluid model simulation at given operating conditions ($U_l = 0.3$ cm/s; $U_g = 6.0$ cm/s) and wetting conditions. Figs. 4 and 5 show contours of solid volume fraction distribution in the model beds (II, III, IV) and the corresponding liquid volume fraction (i.e., *holdup*) distributions. It is clear that the effect of porosity distribution on liquid holdup distribution is significant in the case of non-prewetted beds ($f = 0$). The higher the S.D. of the porosity distribution, the higher the S.D. of liquid holdup distribution. Even for the case of partial particle external wetting this effect still exists, which often occurs in deep trickling flow regime. However, further simulations indicate that such porosity effect could be reduced if the packed-bed operates with completely prewetted particles.

4.4. Correlation development

Based on the presented k-fluid model simulation results, it can be concluded that high heterogeneity of the porosity distribution and high capillary force result in

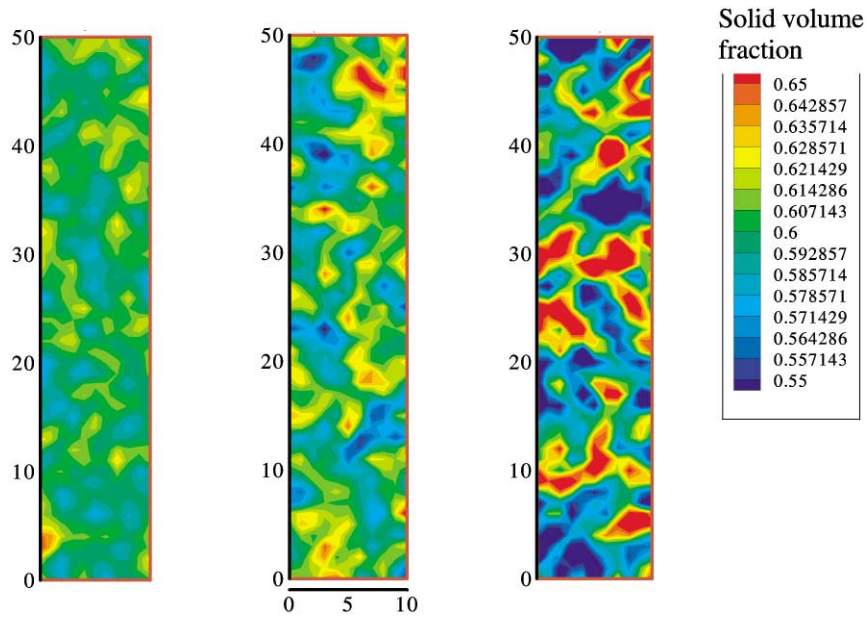

Fig. 4. Contours of solid volume fraction (= 1.0-porosity) distribution in model beds (II, III, IV) for *k*-fluid model simulations.

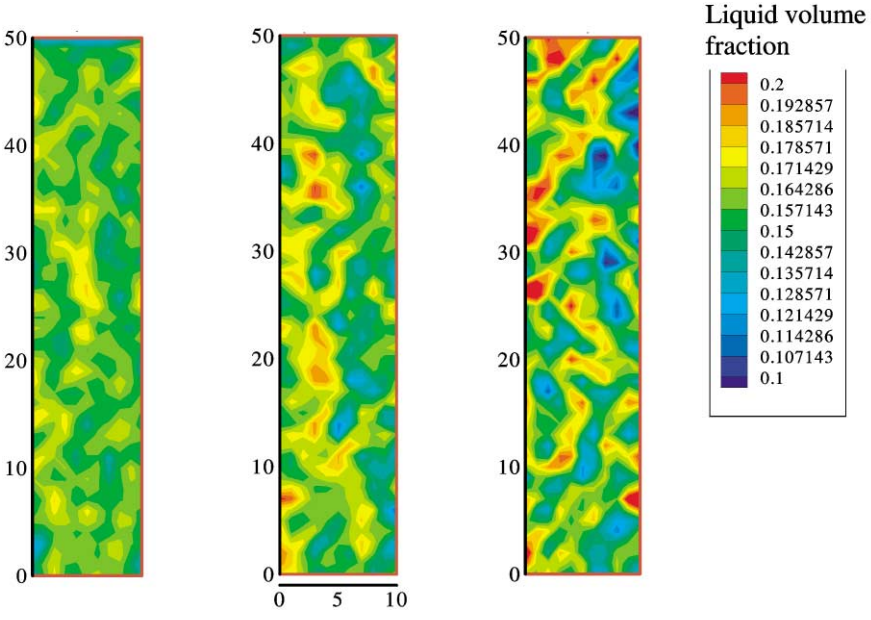

Fig. 5. Contours of *k*-fluid model simulated liquid volume fraction (holdup) distribution in model beds (II, III, IV).

high heterogeneity of liquid holdup and two phase flow velocities. To quantify this relationship of bed structure, particle wetting and resultant flow distribution, we correlate these distribution results in terms of statistical parameters (e.g., standard deviation (S.D.)). For example, we can develop a correlation between the standard deviation of the holdup distribution σ_l, external wetting efficiency, f, and the standard deviation of the bed porosity, σ_B, as given in Eqs. (9)–(10c). Fig. 6 shows the comparison of the *k*-fluid model computed value of the holdup standard deviation, σ_l, with the value calculated from the correlation below:

$$\sigma_l = a_1(\sigma_B)f^2 + a_2(\sigma_B)f + a_3(\sigma_B), \tag{9}$$

$$a_1(\sigma_B) = -0.1696\sigma_B - 0.0002, \tag{10a}$$

$$a_2(\sigma_B) = -0.2593\sigma_B + 0.0012, \tag{10b}$$

$$a_3(\sigma_B) = 0.5002\sigma_B + 0.0019. \tag{10c}$$

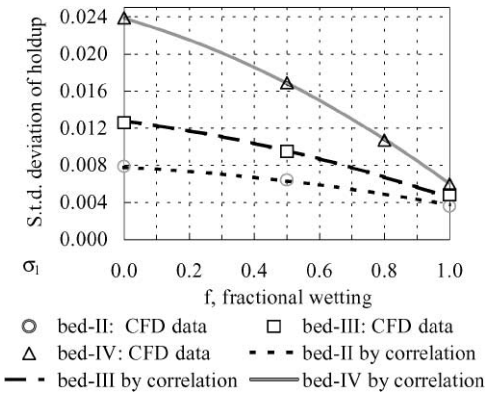

Fig. 6. Standard deviation of the liquid holdup distribution from *k*-fluid model simulations and from Eq. (9) calculations vs. bed wetting factor (f) in model Bed-II–IV.

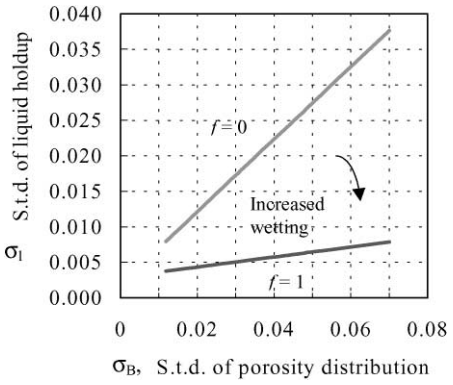

Fig. 7. Standard deviation of the liquid holdup distribution vs. standard deviation of bed porosity at two wetting limits at $U_{l0} = 0.3$ cm/s, and $U_{g0} = 6.0$ cm/s.

With respect to its two limits of the prewetting states (i.e. $f = 0.0$ and 1.0), it is possible to establish Eqs. (11a) and (11b) which correspond to the non-prewetted case and the prewetted case, respectively

$$\sigma_l = 0.5002\sigma_B + 0.0019 \quad (f = 0.0), \tag{11a}$$

$$\sigma_l = 0.0713\sigma_B + 0.0029 \quad (f = 1.0). \tag{11b}$$

The ratio of the slopes of the two straight linear lines (Eqs. (11a) and (b)) is about 7.0 for the given operating condition as plotted in Fig. 7. A higher degree of particle external wetting diminishes the effect of bed structure on two phase flow distribution.

The choice of fractional wetting (f-value) in the *k*-fluid model simulation is very important due to the major effect of fractional wetting on flow distribution. Since the fractional wetting (f) can be described as the percentage of particle external surface covered by continuous liquid film (*unbroken*) in whole packed beds, the particle external wetting efficiency developed in trickle-bed literature can be used as a good approximation of the fractional wetting. One may use the correlation of overall liquid holdup (e.g., Holub et al., 1992) to calculate the mean liquid holdup, and use the correlation for particle external wetting efficiency (e.g., Al-Dahhan et al., 1995) to evaluate f, then use Eq. (9) to calculate the standard deviation of the holdup if σ_l, the standard deviation of porosity σ_B is available for given inflow condition, and eventually establish the Gaussian probability density function (p.d.f.) for liquid-holdup distribution in trickle beds.

4.5. Superficial velocities at the inlet

The above simulation results are given for certain inlet conditions ($U_l = 0.3$ cm/s; $U_g = 6.0$ cm/s). Fig. 8 shows the dependence of the global liquid holdup and particle external wetting efficiency on liquid superficial velocity at gas superficial velocity of 3 cm/s. Particle partial-wetting occurs at the liquid superficial mass velocity less than 6 kg/m^2/s, where both porosity distribution and partial wetting contribute to the two phase flow distribution.

Fig. 9 shows the CFDLIB simulated liquid holdup (mean + S.D.) at different liquid superficial mass velocities. The holdup values calculated by Holub et al. (1992) correlation are also plotted (filled square). Clearly,

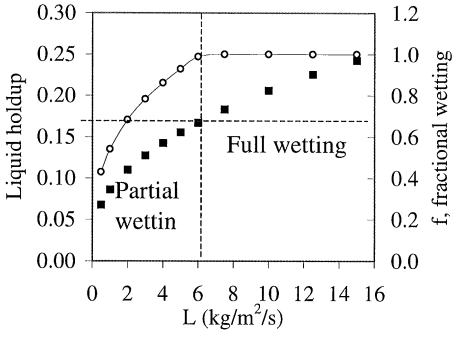

Fig. 8. Liquid holdup (filled squares) (Holub et al., 1992) and particle external wetting efficiency from correlation (empty circle) (Al-Dahhan & Dudukovic, 1995).

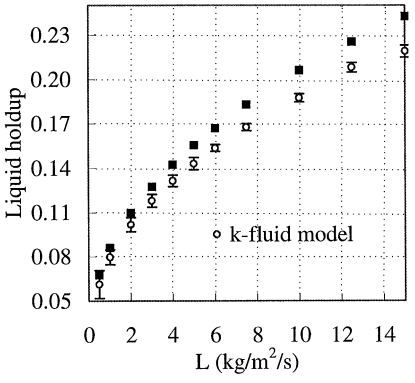

Fig. 9. Liquid holdup values from *k*-fluid model (mean + S.D.) and Holub's slit model (1992): $\varepsilon_B = 0.399$; $d_p = 3$ mm; $U_g = 0.03$ m/s Plus and minus bars are the standard deviation of liquid holdup.

the global holdup correlation gives higher values than those from k-fluid model simulations particularly at high liquid flow rate. One of the reasons could be the use of the global correlation from 3-D beds on the current 2-D model bed which was simulated.

It is interesting to note that the higher values of liquid holdup standard deviation are obtained at low and high liquid superficial mass velocities, and a minimum holdup standard deviation exists at L of 6 kg/m^2/s, where a complete particle external wetting is just reached. Similar experimental observation was reported earlier (Jensen, 1977). In the partial particle external wetting regime, a decrease in liquid superficial velocity a lower in f, and further enhances the capillary force effect, and eventually results in more liquid non-uniformity (e.g. higher standard deviation of liquid holdup). In the fully wetted regime, however, the flow passage size decreases with increasing inlet liquid velocity and, it causes more significant gas–liquid interactions which result in non-uniformities.

5. Concluding remarks

Because of the statistical nature of section-scale porosity distribution in packed-beds, the section-scale gas and liquid distributions in trickle beds has been characterized by pseudo-Gaussian function in which the mean value is evaluated by the global correlation (e.g. Holub et al., 1992), and the standard deviation (S.D.) is estimated based on the S.D.-correlation developed in this study provide that the S.D. of porosity is known. Capillary pressure partially contributes to the liquid distribution if particles are partially wetted by liquid flow. The effect of porosity non-uniformity on liquid distribution is diminished if the particles are fully wetted. CFD is shown to be an efficient numerical tool for developing quantitative relationships among bed structure, particle wetting and operating conditions. Although the present numerical study was limited to a 2-D rectangular bed, the extension to 3-D cylindrical packed-column simulations is in progress. The extensive experimental validations of numerical results using CT and MRI techniques are proposed as future work to establish the final structure-flow correlation.

Notation

d_p	particle diameter, m
E_1, E_2	Ergun constants ($E_1 = 180$; $E_2 = 1.8$)
f	fractional wetting value
$f(x_j)$	probability density function
F_D	Drag force
g	gravity, cm/s^2
P_0	pressure, dyn/cm^2
u_0	material velocity, cm/s
$\lvert u_{kl}\rvert$	slip interstitial velocity between phases k and l, cm/s
$\bar{u}_k$	material k interstitial velocity vector, cm/s
$\bar{u}'_k$	fluctuating part of k interstitial velocity vector, cm/s
V_r	Superficial relative velocity based on gas flow, as defined in Eq. (7d), cm/s
V_x, V_z	interstitial velocity components, cm/s
U_0	input superficial velocity, cm/s
X_{kl}	momentum exchange coefficient between phase k and l
x_j	variable of system

Greek letters

α_1, α_2, α_3	parameters
α_k	material indicator ($=1$ if k is present; $=0$ otherwise)
$\dot{\alpha}_k$	material derivative
ε_B	bed porosity
ε	section porosity
θ_k	material k volume fraction ($\theta_k = \langle\alpha_k\rangle$)
τ_0	deviatiric stress
ρ	density of fluid, kg/m^3 (gas: 1.2; liquid: 1000)
ρ_k	density of material k, g/cm^3 ($\equiv \langle\alpha_k\rho_0\rangle$)
μ	mean value
μ_α	viscosity of phase α
σ_s	surface tension
σ_B	standard deviation of porosity distribution
σ_l	standard deviation of liquid holdup
γ_1	Skewness of statistical data
γ_2	Kurtosis of statistical data
$\langle\ \rangle$	ensemble averaged

Acknowledgements

The authors would like to acknowledge the support provided by the industrial sponsors of the CREL and to thank Dr. M.R. Khadilkar and Dr. S. Kumar for their helpful discussions.

References

Al-Dahhan, M. H., & Dudukovic, M. P. (1995). Catalyst wetting efficiency in trickle-bed reactors at high pressure. *Chemical Engineering Science*, *50*, 2377–2389.

Al-Dahhan, M. H., Khadilkar, M. R., Wu, Y., & Dudukovic, M. P. (1998). Prediction of pressure drop and liquid holdup in high-pressure trickle-bed reactors. *Industrial and Engineering Chemistry Research*, *37*, 793–798.

Attou, A., Boyer, C., & Ferschneider, G. (1999). Modeling of the hydrodynamics of the cocurrent gas-liquid trickle flow through a trickle-bed reactor. *Chemical Engineering Science*, *54*, 785–802.

Baldwin, C. A., Sederman, A., Mantle, M. D., Alexander, P., & Gladden, L. F. (1996). Determination and characterization of the structure of a pore space from 3D volume images. *Journal of Colloid Interface Science*, *181*, 79–92.

Bemer, G. G., & Zuiderweg, F. J. (1978). Radial liquid spread and maldistribution in packed columns under different wetting conditions. *Chemical Engineering Science*, *33*, 1637–1643.

Benenati, R. F., & Brosilow, C. B. (1962). Void fraction distribution in beds of spheres. *A.I.Ch.E. Journal*, *8*, 359.

Bey, O., & Eigenberger, G. (1997). Fluid flow through catalyst filled tubes. *Chemical Engineering Science*, *52*, 1365–1376.

Chen, J., Rodas, N., Al-Dahhan, M. H., & Dudukovic, M. P. (2000). Study of particle motion in packed/ebullated beds by CT and CARPT. *A.I.Ch.E. Journal*, in press.

Crine, M., Marchot, P., & L'Homme, G. (1992). Statistical hydrodynamics in trickle flow columns. *A.I.Ch.E. Journal*, *38*, 136–147.

Grosser, K. A., Carbonell, R. G., & Sundaresan, S. (1988). Onset of pulsing in two-phase cocurrent downflow through a packed bed. *A.I.Ch.E. Journal*, *34*, 1850.

Hoek, P. J., Wesselingh, J. A., & Zuiderweg, F. J. (1986). Small scale and large scale liquid maldistribution in packed columns. *Chemical Engineering Research Design*, *64*, 431–449.

Holub, R. A., Dudukovic, M. P., & Ramachandran, P. A. (1992). A phenomenological model for pressure-drop, liquid holdup, and flow regime transition in gas-liquid trickle flow. *Chemical Engineering Science*, *47*, 2343–2348.

Holub, R. A., Dudukovic, M. P., & Ramachandran, P. A. (1993). Pressure drop, liquid holdup, and flow regime transition in gas-liquid trickle flow. *A.I.Ch.E. Journal*, *39*, 302–321.

Jensen, R. H. (1977). Optimum liquid mass flux for two phase flow through a fixed bed of catalyst. US4039430.

Jiang, Y., Khadilkar, M. R., Al-Dahhan, & Dudukovic, M. P. (1999). Two phase flow distribution in 2D trickle bed reactors. *Chemical Engineering Science*, *54*, 2409–2419.

Jiang, Y., Khadilkar, M. R., Al-Dahhan, & Dudukovic, M. P. (2000). Single phase flow modeling in packed beds: A discrete cell approach revisited. *Chemical Engineering Science*, *55*, 1829–1844.

Jodrey, W. S., & Tory, E. M. (1981). Computer simulation of isotropic, homogeneous, Dense random packing of equal spheres. *Power Technology*, *30*, 111–118.

Jolls, K. R., & Hanratty, T. J. (1966). Transition to turbulence for flow through a dumped bed of spheres. *Chemical Engineering Science*, *21*, 1185–1190.

Kashiwa, B. A., Padial, N. T., Rauenzahn, R. M., & Vander Heyden, W. B. (1994). A cell centered ICE method for multiphase flow simulations. *ASME symposium on numerical methods for multiphase flows*, Lake Tahoe, Nevada.

Khadilkar, M. R. (1998). *Performance studies of trickle-bed reactors*. Doctoral Thesis, Washington University, St. Louis, MO., USA.

Kumar, S. (1995). Simulation of multiphase flow system using CFDLIB code. *CREL Annual Meeting Workshop*, St. Louis, MO., USA.

Latifi, M. A., Midoux, N., & Storck, A. (1989). The use of micro-electrodes in the study of the flow regimes in packed bed reactor with single phase liquid flow. *Chemical Engineering Science*, *44*, 2501–2508.

Levec, J., Grosser, K., & Carbonell, R. G. (1988). The hysteretic behavior of pressure drop and liquid holdup in trickle beds. *A.I.Ch.E. Journal*, *34*, 1027–1030.

Levec, J., Saez, A. E., & Carbonell, R. G. (1986). The hydrodynamics of trickling flow in packed beds: Experimental observations. *A.I.Ch.E. Journal*, *32*, 369.

Logtenberg, S. A., & Dixon, A. G. (1998). Computational fluid dynamics studies of the fixed bed heat transfer. *Chemical Engineering Processing*, *37*, 7–21.

Lutran, P. G., Ng, K. M., & Delikat, E. P. (1991). Liquid distribution in trickle beds. An experimental study using computer-assisted tomography. *Industrial and Engineering Chemistry Research*, *30*, 1270.

Melli, T. R., Santos, J. M., Kolb, W. B., & Scriven, L. E. (1990). Cocurrent downflow in networks of passages: Microscale roots of macroscale flow regimes. *Industrial and Engineering Chemistry Research*, *29*, 2367–2379.

Melli, T. R., & Scriven, L. E. (1991). Theory of two-phase cocurrent downflow in networks of passages. *Industrial and Engineering Chemistry Research*, *30*, 951–969.

Mueller, G. E. (1991). Prediction of radial porosity distribution in randomly packed fixed beds of uniformly sized spheres in cylindrical containers. *Chemical Engineering Science*, *46*, 706.

Nijemeisland, M., Logtenberg, A. A., & Dixon, A. (1998). FD studies of wall-region fluid flow and heat transfer in a fixed bed reactor. *A.I.Ch.E. Annual Meeting*, Paper 311f, Miami, FL.

Ravindra, P. V., Rao, D. P., & Rao, M. S. (1997). Liquid flow texture in trickle-bed reactors: An experimental study. *Industrial and Engineering Chemistry Research*, *36*, 5133.

Reinecke, N., Petritsch, G., Schmitz, D., & Mewes, D. (1998). Tomographic measurement techniques: Visualization of multiphase flows. *Chemical Engineering Technology*, *21*, 7–18.

Roussas, G. G. (1997). *A course in mathematical statistics* (2nd ed.). New York: Academic Press.

Saez, A. E., & Carbonell, R. G. (1985). Hydrodynamic parameters for gas-liquid cocurrent flow in packed beds. *A.I.Ch.E. Journal*, *31*, 52–62.

Sederman, A. J. (2000). PDF of voxel porosity distribution. *Personal Communication*, from University of Cambridge.

Sederman, A. J., Johns, M. L., Bramley, A. S., Alexander, P., & Gladden, L. F. (1997). Magnetic resonance imaging of liquid flow and pore structure within packed beds. *Chemical Engineering Science*, *52*, 2239–2250.

Song, M., Yin, F. H., Chuang, K. T., & Nadakumar, K. (1998). A stochastic model for the simulation of the natural flow in random packed columns. *The Canadian Journal of Chemical Engineering*, *76*, 183–189.

Toye, D., Marchot, P., Crine, M., & L'Homme, G. (1997). Computer-assisted tomography for liquid imaging in trickle flow columns.. In J. Chaouki, F. Larachi, & M. P. Dudukovic (Eds.), *Non-invasive monitoring of multiphase flows* (p. 105). Amsterdam: Elsevier.

Volkov, S. A., Reznikov, V. I., Khalilov, K. F., Zel'vensky, Yu. V., & Sakodynsky, K. I. (1986). Nonuniformity of packed beds and its influence on longitudinal dispersion. *Chemical Engineering Science*, *41*, 389.

Wang, Y. -F., Mao, Z. -S., & Chen, J. (1998). Scale and variance of radial liquid maldistribution in trickle beds. *Chemical Engineering Science*, *53*, 1153–1162.